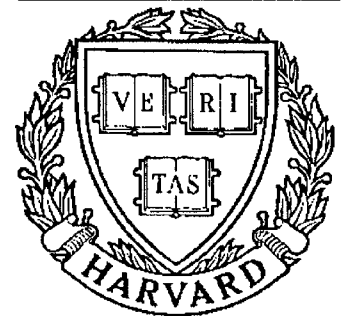


TECHNICAL RESEARCH REPORT



S Y S T E M S
R E S E A R C H
C E N T E R



*Supported by the
National Science Foundation
Engineering Research Center
Program (NSFD CD 8803012),
Industry and the University*

Simulation of Surface Topography Formed During the Intermittent Turning Processes

*by G.M. Zhang, S. Yerramareddy,
S.M. Lee, and S.C-Y. Lu*

Simulation of Surface Topography Formed during the Intermittent Turning Processes

G. M. Zhang

Department of Mechanical Engineering and Systems Research Center
University of Maryland
College Park, MD 20742

S. Yerramareddy, S. M. Lee, and S. C-Y. Lu

Knowledge-Based Engineering Systems Research Laboratory
Department of Mechanical and Industrial Engineering
University of Illinois at Urbana-Champaign
1206 West Green Street
Urbana, IL 61801

Abstract

This paper presents a methodology which employs computer simulation to dynamically generate the topography of a surface machined during an intermittent turning process. The methodology is based on a mathematical model that characterizes the intermittent turning process as an alternating sequence of forced and free vibratory motion. The simulation of machining workpieces, with discontinuous geometries of arbitrary shape, is facilitated by representing the workpiece surface as a two-dimensional grid, with an index for each cell in the grid accounting for the feature boundaries. The tool vibratory motion is integrated with the tool geometric motion to form a basis for the construction of surface texture produced during machining. The simulation model not only provides for a qualitative evaluation of the surface accuracy through a graphic visualization of the surface topography, but also provides a quantitative estimate of the roughness quality of the machined surface.

1. Introduction

Control of surface accuracy during machining has attracted great attention in recent times. Complex parts with discontinuous geometries aggravate the problem of controlling the surface accuracy. These discontinuous geometries alter the cutting dynamics of the machining process. When machining cylindrical parts with discontinuous surface features such as holes and slots on the circumference, the

cutting tool is engaged in machining intermittently. Figure 1 gives a sketch of an intermittent turning process.

Controlling surface accuracy essentially involves the control of both the static and the dynamic tool path errors. Highly accurate spindle and straight feed mechanisms are being used to reduce the static part of the tool path error during machining. Adaptive control systems that correct the dynamic tool path errors based on the in-process measurement of the workpiece surface have been used to achieve higher levels of accuracy [1]. This approach to the control of the dynamic tool path errors relies on the modeling of the cutting dynamics of the machining process [2,3]. However, this and similar approaches do not lend themselves well to the control of intermittent turning processes, because the presence of discontinuous geometries introduces problems in the in-process tracking of the tool path. In addition, the presence of discontinuous geometries often leads to sudden tool breakage. Therefore, there is a need for the off-line evaluation of the intermittent turning process.

A simulation model has recently been developed to study the dynamic characteristics of the intermittent turning process [4]. It was proposed that during intermittent machining, the cutting tool is alternatively subjected to forced and free vibratory motion. The random tool path error was modeled in terms of a random excitation due to the non-homogeneous hardness distribution in the material being machined. The model, however, was based on several simplifying assumptions.

The work presented in this paper is a continuation of the study of the cutting dynamics during the intermittent turning process. Several of the key assumptions are relaxed. The regenerative mechanism (overlap cutting) is incorporated in the current simulation model. In order to account for discontinuous geometries of arbitrary shape, the workpiece surface is being represented in terms of a two-dimensional grid, with an index for each cell in the grid representing the boundaries of the discontinuous features on the surface. Practical performance criteria such as the surface roughness

measure have been included in the model. A method to construct the three-dimensional topography of a machined surface has been incorporated to provide for better visualization.

The rest of the paper is organized into the following sections. In section 2, the simulation methodology is described. Section 3 outlines the various case studies that were performed and the criteria used to evaluate the simulation results. The effects of the shape and size of the discontinuities as well as the cutting parameters on the machining accuracy are discussed in section 4. The significance of the simulation results is also discussed.

2. Simulation Methodology

The block diagram depicting the simulation model for generating the machined surface topography is shown in Fig. 2. The simulation model consists of the following four modules: the input function module, the machining system module, the tool geometric motion module, and the surface topography generation module. The first two modules constitute the model of the intermittent turning process. The output of this model is the tool vibratory motion, which is integrated with the tool geometric motion to generate the surface topography. The details of these modules are discussed in the subsequent sections.

2.1 Machining System Model

The machining system is modeled as consisting of two sub-systems, the cutting process and the machine tool structure, with a feedback mechanism linking the cutting process and the machine tool structure. Only a brief outline of the model will be presented here, and a more detailed discussion of the model can be found elsewhere [4,5].

The system model is based on some simplifying assumptions.

1. It is assumed that the rigidity of the machine tool as well as the workpiece are much greater than the rigidity of the toolpost. For this assumption to be valid, the length to diameter ratio of the workpiece should be small.
2. The magnitude of the tool vibration is assumed to be small compared to the depth of cut. This assures that the tool point never leaves the workpiece surface during the cutting period, making it possible to use a linear system model.

A second-order model, as shown in Fig. 3, is used to represent the dynamics of the toolpost structure on which the cutting tool is firmly supported. The mathematical form of this model is given by

$$M \frac{d^2[y(t)]}{dt^2} + C \frac{d[y(t)]}{dt} + K[y(t)] = F \cdot \cos \theta \quad (1)$$

where

M = lumped mass of the toolpost structure,

C = damping factor of the toolpost structure,

K = static stiffness of the toolpost structure, and

F = cutting force, and

$F \cos \theta$ = component of the force along a direction normal to the machined surface.

The cutting force in this equation is contributed by the chip load which is comprised of three components, namely the nominal chip load, the random excitation and the chip load differential due to feedback.

2.1.1 Chip Load and Cutting Force

The nominal chip load is the average chip load on the tool. It is determined by the feed and the depth of cut and remains constant, as long as the cutting parameters do not change. If the cutting process is continuous, the nominal chip load can be represented by a step function, the magnitude of which is equal to the product of feed and depth of cut, or alternatively the product of width of cut and thickness of cut, as indicated in Fig. 1. During an intermittent turning process, the magnitude of this step function as calculated above is valid only during the cutting period. It, however, drops to zero when the tool passes over the discontinuity, which constitutes the non-cutting period. The nominal chip load can be expressed as

$$\text{nominal chip load} = \begin{cases} (f \cdot d) \text{ or } (w \cdot a) & \text{cutting period} \\ 0 & \text{non-cutting period} \end{cases} \quad (2)$$

where

f = feed

d = depth of cut

w = width of cut = $d/\cos C_s$,

a = thickness of cut = $f \cos C_s$, and

C_s = lead angle of tool.

It has been observed that the cutting tool is subjected to random excitation during machining. The major source of random excitation is attributed to the nonhomogeneous hardness distribution in the workpiece material being machined [6]. The hardness distribution, and consequently the chip load variation, in general, follows a normal distribution. The random component of the chip load is given by [7]

$$\text{random chip load} = w \cdot a \cdot \left[\left(\frac{\mu_s(t)}{\mu_a} \right)^m - 1 \right] \quad (3)$$

where

μ_a = average hardness of the material being cut,

$\mu_s(t)$ = hardness of the grid being cut at time, t ,

m = Meyer exponent that explains the nonlinear relation between the chip load and the hardness ratio, $\mu_s(t)/\mu_a$.

The hardness, $\mu_s(t)$ is measured at points along the circumference of the workpiece using a microhardness tester, as explained in [7]. The hardness distribution has to be established for different materials and heat treatments.

The chip load differential due to feedback is comprised of two components. The primary chip load variation is caused by the tool vibration during machining [5], and is given by

$$\text{primary chip load variation} = -w \cdot y(t) \quad (4)$$

where $y(t)$ represents the change in position of the tool due to vibration, as indicated in Fig. 1. The variation of the chip load from the nominal caused by the tool vibratory motion results in an uneven machined surface. The surface modulations during any particular revolution will affect the chip load during the subsequent revolution. This variation of chip load is called the regenerative chip load variation [5]. Considering this variation indicates that the system model used in the present work takes into account the effect of self-excitation on the evaluation of the tool vibratory motion during machining. This variation is given by

$$\text{regenerative chip load variation} = w \cdot \Delta y(t-T) \cdot \mu = w \cdot [y(t-T) - y_{\text{equilibrium}}] \cdot \mu \quad (5)$$

where

$\Delta y(t-T)$ = regenerative chip load at cutting instant t ,

$y(t-T)$ = magnitude of tool vibration at cutting instant $(t-T)$

$y_{\text{equilibrium}}$ = dynamic equilibrium position of tool during the previous revolution of workpiece,

T = time needed for one revolution of workpiece, and

μ = magnification factor of the regenerative feedback loop.

The magnification factor of the regenerative feedback loop, μ , reflects the degree of overlap between the adjacent cuts (for example, $\mu = 1$ for plunge cutting, and $\mu = 0$ for thread cutting). Methods to determine this magnification factor can be found in [8].

The chip load variation during machining, due to both the primary and the regenerative feedback together, is given by

$$\text{total chip load variation} = -w \cdot y(t) + w \cdot \Delta y(t-T) \cdot \mu \quad (6)$$

The cutting force contributed by these three components of the chip load is given by

$$F = K_a \cdot (w \cdot a) + K_a \cdot w [\Delta y(t-T) \cdot \mu - y(t)] + K_a \cdot w \cdot a \cdot \left[\left(\frac{\mu_s(t)}{\mu_a} \right)^m - 1 \right] \quad (7)$$

where K_a is the unit cutting force, a proportionality coefficient determined mainly by the material being machined.

2.1.2 Simulation Model

As described earlier, the system is subjected to forced vibratory motion during the cutting period, where the cutting force acts as the forcing function. In addition, the system is also subjected to a self-excitation due to the regenerative mechanism (overlap cutting). However, when the cutting tool passes over a discontinuity (non-cutting period), the chip load and hence the cutting force becomes zero, thus subjecting the system to free vibratory motion. Combining these two cases, along with the associated initial conditions, the simulation model is given by

$$\text{Simulation Model} = \left\{ \begin{array}{l} \text{Cutting Period:} \\ \\ M \frac{d^2[y(t)]}{dt^2} + C \frac{d[y(t)]}{dt} + K[y(t)] = \\ K_a \cdot w \cdot \{[a - y(t)] + \mu \Delta y(t-T)\} + a \cdot \left[\left(\frac{\mu_s(t)}{\mu_a} \right)^m - 1 \right] \cos \theta \\ y(t)|_{t=0} = 0 \quad \text{and} \quad \dot{y}(t)|_{t=0} = 0 \quad \text{or} \\ y_{\text{free}}(T_1 + 0) = y_{\text{forced}}(T_1) \\ \dot{y}_{\text{free}}(T_1 + 0) = \dot{y}_{\text{forced}}(T_1) \\ \\ \text{Non-Cutting Period:} \\ \\ M \frac{d^2[y(t)]}{dt^2} + C \frac{d[y(t)]}{dt} + K[y(t)] = 0 \\ \\ y_{\text{forced}}(T_2 + 0) = y_{\text{free}}(T_2) \\ \dot{y}_{\text{forced}}(T_2 + 0) = \dot{y}_{\text{free}}(T_2) \end{array} \right. \quad (8)$$

where

T_1 = time duration of the cutting period, and

T_2 = time duration of the non-cutting period.

The initial conditions indicate that the displacement and velocity of the tool vibratory motion at the end of the cutting period serve as the initial conditions for the evaluation of the tool motion during the non-cutting period, and vice versa. The machining system module uses the analytical solutions of the simulation model. The derivation of the analytical solutions is described elsewhere [4].

2.1.3 Workpiece Surface Representation

As indicated by Eq. (8), the system equation is dependent on whether it is in the free vibration mode (non-cutting period) or the forced vibration mode (cutting period). A way of differentiating the cutting and the non-cutting periods is, therefore, needed. In order to accommodate discontinuities of arbitrary shape, the workpiece surface is represented as a two-dimensional rectangular grid. For example, the surface of the cylindrical part shown in Fig. 4a is represented as shown in Fig. 4b.

The two dimensions of the rectangular grid represent the circumference of the workpiece (in the direction of cutting speed) and the cut length (in the direction of feed), respectively. The grid spacing in the direction of feed is equal to the feed. In the circumferential direction, the resolution and the frequency of vibration guide the selection of the spacing. If the circumference is divided into NUM number of divisions, the grid spacing is given by $(\pi D/\text{NUM})$. Each cell in the grid is assigned a boolean index, which takes a value of one or zero, depending on whether it forms part of the material or the discontinuity. Since a curvilinear discontinuity cannot be accurately represented by rectangular cells, it has to be assumed that a cell forms part of the material, even if it is partially filled, as shown in Fig. 4c. However, a finer cell size would alleviate the inaccuracy caused due to this assumption.

2.2 Surface Topography Generation

The topography of the machined surface is a result of three independent motions along three perpendicular directions, namely

- the rotatory motion of the workpiece,
- the translatory motion of the tool, and
- the vibratory motion of the tool.

The rotatory motion of the workpiece is a function of the cutting speed and can alternatively be represented as a translatory motion of the tool along the circumference of the workpiece. The translatory motion of the tool along the the workpiece axis is a function of the feed. The combined motion of the tool along the feed and the speed directions is generally called the tool geometric motion. The tool geometric and vibratory motions, together, control the position of the tool point during machining. Hence the generation of surface topography requires an integration of the tool geometric and vibratory motions.

The determination of the tool geometric motion is based on the following three assumptions.

1. The tool point is part of a circle of radius R .
2. The roughness profiles are solely made of a series of arc segments.
3. The effective rake angle of the tool is equal to zero degrees.

The generation of a three-dimensional surface topography progresses in two steps. First, two-dimensional profiles along the workpiece axis are generated. Then, the two-dimensional profiles are put together to form the three-dimensional topography of the machined surface.

As indicated in Fig. 5, the construction of a two-dimensional roughness profile hinges on the determination of the coordinates of the centers of arc segments and the points of intersection between two neighboring arc segments. The x-coordinates of successive arc centers are incremented by feed, whereas the y-coordinate is determined by the tool vibratory motion, and is measured from a reference surface determined by the depth of cut. The coordinates of the points of intersection are determined by the coordinates of the centers of the two neighboring arc segments, and the tool radius. As shown in Fig. 5, they are given by

$$\begin{aligned}x_1 &= X_1 + R \cdot \cos\phi \\y_1 &= Y_1 + R \cdot \sin\phi\end{aligned}\tag{9}$$

where X_1 = x-coordinate of the first arc center,
 Y_1 = y-coordinate of the first arc center, and
 R = nose radius of the cutting tool.

3. Simulation of Surface Topography

Several case studies were performed to study the effects of the discontinuities on the surface accuracy in the present work. The simulation conditions are given in Table 1. The surface topographies generated were evaluated both qualitatively and quantitatively. The qualitative evaluation is facilitated by the graphic visualization of the three-dimensional surface topography.

Surface roughness index (AA) has been used to quantitatively characterize the surface texture formed during machining. By definition, the AA value is given by

$$AA = \frac{\sum_{i=1}^p |y_i - \bar{y}|}{p}\tag{10}$$

where y_i = profile height at the i^{th} location,

\bar{y} = mean value of profile heights, and

p = number of peaks used in the evaluation.

It has to be noted that the calculated (or measured) AA value varies with the location on the machined surface. For a better evaluation, it is necessary to take a few roughness profiles and estimate the mean and the associated standard deviation, which can be calculated as follows.

$$AA_{\text{mean}} = \frac{1}{h} [AA_1 + AA_2 + \dots + AA_h]$$

$$S_{AA} = \sqrt{\frac{1}{h} \sum_{i=1}^h (AA_i - AA_{\text{mean}})^2} \quad (11)$$

where h = number of roughness profiles evaluated.

The following parameter settings were used in the case studies. They were based on the data and experimental results presented in [2].

For the machine tool:

static stiffness $K = 1.0 \times 10^6$ N/m

equivalent mass $M = 0.7$ kg.

damping factor $C = 140$ rad/sec.

For the workpiece:

material = 1040 steel.

unit cutting force $K_a = 2.0 \times 10^9$ N/m².

mean of hardness distribution $\mu_a = 175$ (BHN).
variance of hardness distribution $\sigma_s^2 = 172$ (BHN)².

Meyer exponent $m = 0.454$.

For the cutting tool:

lead angle $C_s = 30$ degrees

4. Results and Discussion

4.1 Effect of the Geometry and the Cutting Parameters

Figure 6a shows the surface topography generated during a continuous turning process (case 1). Since there are no discontinuities on the surface, the surface irregularities shown in Fig. 6a are mainly due to the chip load variation through the primary and regenerative feedback paths, and the random excitation due to the nonhomogeneous distribution of microstructures in the material being cut. The AA_{mean} value, based on the topography shown in Fig. 6a, is equal to 15 μm and the associated standard deviation is equal to 1.2 μm .

In order to study the effect of discontinuous geometries on the machined surface topography, the results of case 1 are compared with those of case 2. Case 2 involves the machining of a workpiece with discontinuous geometry. The discontinuity is a rectangular hole on the circumference of the workpiece as shown in Table 1. Figure 6b shows the topography generated for case 2. The simulation conditions used are identical to those used in case 1 except for the presence of the discontinuous geometry in case 2. The major difference between the two topographies (Fig. 6a and Fig. 6b) is the presence of a hill along the edge of the rectangular hole. This hill is a result of the sudden application of the nominal chip load at the beginning of each cutting period. The sudden impact pushes the tool away from the workpiece, leaving part of the material uncut to form the hill on the machined surface. It is obvious that this

hill degrades the surface finish severely. The roughness profile shown in Fig. 7a, which is taken from the topography shown in Fig. 6b, consists of two distinct parts, one from the region before the discontinuity and the other in the vicinity of the discontinuity. The mean line shown in Fig. 7a is significantly tilted, thus leading to a large AA value. It is interesting to note that, as indicated in Fig. 7b, calculations based on the simulation data indicate that there is no significant difference between the AA value measured in the vicinity of the discontinuity (15.2 μm) and the AA value measured in regions away from the discontinuity (15.0 μm). Therefore, the quantity which affects the AA measurement is the shift of the mean line from a lower level to a higher level, as indicated in Fig. 7b. This shift can be calculated as follows.

$$\begin{aligned}\text{shift of mean line} &= \bar{y}_i - \bar{y}_c \\ &= 719 - 697 = 22 \text{ (}\mu\text{m)}\end{aligned}\tag{12}$$

where \bar{y}_i and \bar{y}_c are the mean values of the profile heights in the region of the discontinuity and away from the discontinuity, respectively.

It is evident that in case 2, the shift of the mean line is due to the sudden impact between the tool and the workpiece at the beginning of each cutting period, because the time duration of the non-cutting period seems long enough to damp out the free-vibration of the tool. However, when the time duration of a non-cutting period is short, the effect of the free-vibration of tool can also be observed. Case 3 and case 4 are two typical examples. In case 3, the time duration of the non-cutting period is shortened by one third because the length of the rectangular hole is reduced from 30 mm to 20 mm. Otherwise, the simulation conditions in case 2 and case 3 are identical. Comparing the two topographies shown in Fig. 6b and Fig. 6c, there is a significant shift in the mean level in Fig. 6c (26 μm) compared to that in Fig. 6b (22 μm). Similarly, in case 4, the time duration of the non-cutting period is shortened by half because the spindle

speed has increased from 600 rpm to 1200 rpm. The shift of the mean line shown in Fig. 6d (35 μm), accordingly, is the largest among the three intermittent machining cases.

Due to the complexity of the intermittent turning process, the relation between the shift of the mean line and the time duration of the non-cutting period is not a simple linear relation. Table 2 lists values for the shift of the mean line at different spindle speeds calculated from the simulation results. They indicate a general trend that the higher the spindle speed, the larger the shift of the mean line. However, the shift of the mean line fluctuates at high spindle speeds. For example, it reaches 30 μm at a spindle speed of 800 rpm, but drops as the spindle speed increases further. This is caused by the fluctuation of the initial displacement and velocity at the beginning of the cutting period, which are actually determined by the status of the free-vibration of the tool during the preceding non-cutting period. This points out the importance of proper selection of the spindle speed for the control of machining accuracy during the intermittent turning process.

The topography shown in Fig. 8 represents the intermittent turning process shown in Fig. 1 where a cylindrical hole is located on the circumference of the workpiece. Due to the geometry of the circle, the time duration of the non-cutting period varies along the different cross-sections. The variation of the heights of the hilly pattern clearly indicates the effect of the free-vibration of the tool on the surface texture generation. Along the extremes of the circle, the shift of the mean line is very large because of the very short time duration of the non-cutting period. In the region half-way between the extremes, the shift of the mean line is significantly small because of the longer time duration of the non-cutting period.

4.2 Significance of the Simulation Results

It was alluded to earlier that there are certain practical difficulties in measuring the surface characteristics during intermittent machining. As demonstrated in the previous discussion, the characteristics of the surface around a discontinuous geometry are different from the characteristics of the surface away from the discontinuous geometry. Figure 9 shows a photomicrograph of the machined surface in the vicinity of a discontinuity. This is quite similar to the simulated surface topographies. In addition to the surface waviness, the photograph also reveals the presence of a ridge along the boundary of the discontinuity. In practice, this may raise a question about where to take the profilometer traces and how to deal with the variation among the measured AA values taken from the same machined surface. The present study provides an effective method to solve some of these difficulties. Once the simulator is calibrated, it can substitute for the physical measurement of the surface roughness. Since the topography of the machined surface can be graphically displayed, some of the difficulties described above can easily be overcome. Also, because of the availability of the numerical database generated for the topography construction, surface profiles at specified locations can be constructed with ease. This enables the detection of the indices like the shift of the mean line.

5. Conclusions

A comprehensive model of the intermittent turning process that accounts for the regenerative mechanism (overlap cutting) and the random excitation present during machining has been developed. By integrating the tool vibratory motion with the tool geometric motion, a methodology for the dynamic generation of the topography of the machined surface has been developed.

By representing the workpiece surface by a two-dimensional grid, the simulation model can deal with discontinuous geometries of arbitrary shape. It provides both a

qualitative evaluation through graphic display of the three-dimensional topography, and a quantitative evaluation by calculating the surface roughness indices.

The effect of shape and size of the discontinuities and the cutting parameters on the cutting dynamics has been studied. The relationship between the cutting dynamics and the surface characteristics has also been established. Based on the qualitative and quantitative evaluation of the surface characteristics from the case studies, it was shown that proper selection of spindle speed is critical for the control of machining accuracy during the intermittent turning process.

Acknowledgments

The authors acknowledge the support of the Systems Research Center at the University of Maryland at College Park under Engineering Research Centers Program: NSFD CDF 8803012. Part of the funding for this research is provided by the Digital Equipment Corporation and the University of Illinois Research Board. The authors wish to thank them for their support. Special thanks are due Ms. X. H. Song at the National Center for Supercomputing Applications for her valuable help in preparing some of the graphics.

References

1. T. Kohno, Y. Okazaki, N. Pzawa, K. Mitui, and M. Omoda, "In-Process Measurement and a Workpiece-Referred Form Accuracy Control

- System (WORFAC): Concept of the Method and Preliminary Experiment," Journal of Precision Engineering, Volume 11, Number 1, January 1989, pp. 9-14.
2. S. G. Kapoor, F. Ding, G. M. Zhang, and R. E. DeVor, "A Time-Varying Parameter Model for the Stability Analysis of Intermittent Turning Process," Proceedings of the 13th North American Manufacturing Research Conference, May 1985, pp. 551-557.
 3. M. Anjanappa, J. A. Kirk, and D. K. Anand, "Tool Path Error Control in Thin Rib Machining," Proceedings of the 15th North American Manufacturing Research Conference, May 1987, pp. 485-492.
 4. G. M. Zhang, S. Yerramareddy, S. M. Lee, and S. C-Y. Lu, "Simulation of Intermittent Turning Processes," to be presented at the 1989 Winter Annual Meeting of the ASME, "Control Issues in Manufacturing Processes."
 5. H. E. Merritt, "Theory of Self-Excited Machine-Tool Chatter," Journal of Engineering for Industry, Trans. ASME, Vol. 87, November 1965, pp. 447-454.
 6. G. M. Zhang, and S. G. Kapoor, "Dynamic Generation of Machined Surface," submitted to Journal of Engineering for Industry for review, February 1989.
 7. G. M. Zhang, "Dynamic Modeling and Dynamic Analysis of the Boring Machining System," Ph.D. Thesis, University of Illinois at Urbana-Champaign, U.S.A., January 1986.
 8. G. M. Zhang, S. G. Kapoor, and R. E. DeVor, "A Method to Control Three-Dimensional Stability Border Surfaces," Proceedings of the 15th North American Manufacturing Research Conference, May 1987, pp. 593-599.

NOMENCLATURE

AA	=	surfacer roughness index
AA _{mean}	=	mean value of the AA values calculated from a simulated topography
a	=	thickness of cut during the cutting period
BHN	=	Brinell hardness number
C	=	damping factor used in the toolpost structural model
C _s	=	lead angle of tool
d	=	depth of cut, cutting parameter
F	=	cutting force
f	=	feed, cutting parameter
i	=	an index
K	=	static stiffness of the toolpost structure
K _a	=	unit cutting force
K _m	=	magnification factor
M	=	equivalent mass of the toolpost structure
m	=	Meyer exponent used to evaluate the random part of cutting force
N	=	spindle speed, rpm
NUM	=	number of divisions along the circumference of workpiece
R	=	nose radius of tool
S _{AA}	=	standard deviation associated with AA _{mean}
T	=	time needed for one revolution of workpiece
T ₁	=	time duration of the cutting period
T ₂	=	time duration of the non-cutting period
w	=	width of cut
X	=	x-coordinate of the arc center in a roughness profile
Y	=	y-coordinate of the arc center in a roughness profile

- $y(t)$ = displacement of tool vibratory motion in the direction normal to the machined surface
- $y(t-T)$ = magnitude of tool vibration at cutting instant $(t-T)$
- y_i = profile height at the i^{th} location
- $y_{\text{equilibrium}}$ = dynamic equilibrium position of tool during the previous revolution of workpiece
- $y_{\text{free}}(t)$ = displacement of tool vibratory motion in the direction normal to the machined surface during the non-cutting period
- $y_{\text{forced}}(t)$ = displacement of tool vibratory motion in the direction normal to the machined surface during the cutting period
- $\dot{y}_{\text{free}}(t)$ = velocity of tool vibratory motion in the direction normal to the machined surface during the non-cutting period
- $\dot{y}_{\text{forced}}(t)$ = velocity of tool vibratory motion in the direction normal to the machined surface during the cutting period
- \bar{y} = mean value of profile heights
- \bar{y}_c = mean value of the profile heights of a profile taken in the region of the discontinuity
- \bar{y}_i = mean value of the profile heights of a profile taken in the region away from the discontinuity
- Δt = uniform time interval used in simulation
- $\Delta y(t-T)$ = regenerative chip load at cutting instant t
- μ = magnification factor of the regenerative feedback loop
- μ_a = mean of hardness variation
- μ_s = hardness value at individual cutting locations
- θ = projection angle of the cutting force with respect to the direction normal to the machined surface

ϕ = angle used to evaluate the coordinates of intersection points in a roughness profile

List of Figures

Fig. 1 Intermittent Turning Process

Fig. 2 Methodology to Simulate the Topography of a Machined Surface

Fig. 3 Machining System Model

Fig. 4 Grid Generator

Fig. 5 Construction of a Two-Dimensional Roughness Profile

Fig. 6 Topographies Simulated in the Four Case Studies

Fig. 7 Characteristics of Surface Finish after the Intermittent Turning

Fig. 8 Topography Simulated in Case 5 where a Cylindrical Hole is Located on the Circumference of the Workpiece

Fig. 9 Ridges Formed along the Boundary of Discontinuous Geometry Observed from Experiment (Magnified 28X)

List of Tables

Table 1 Simulation Conditions Used in the Case Studies

Table 2 Shift of Mean Line at Different Spindle Speeds

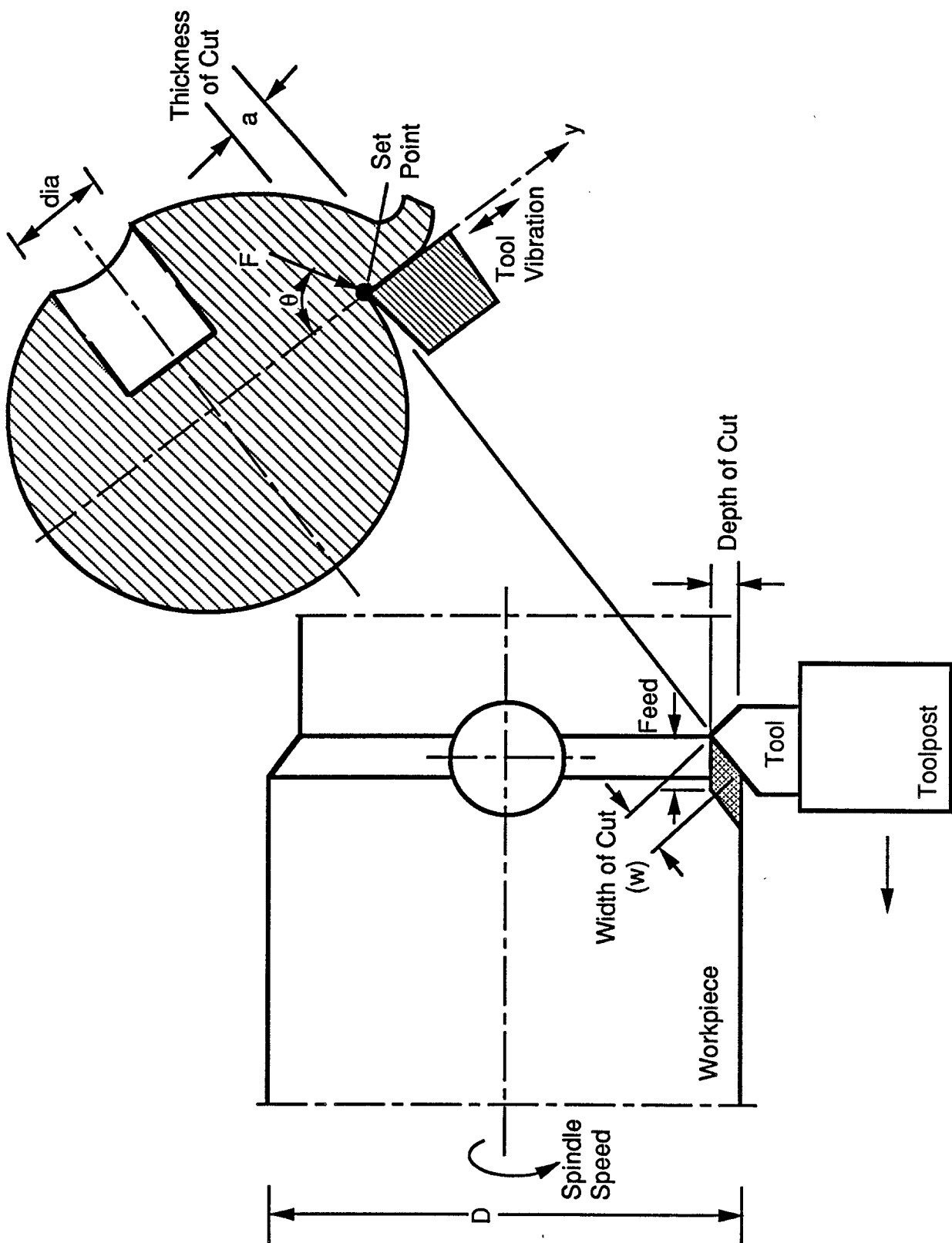


Fig. 1 Intermittent Turning Process

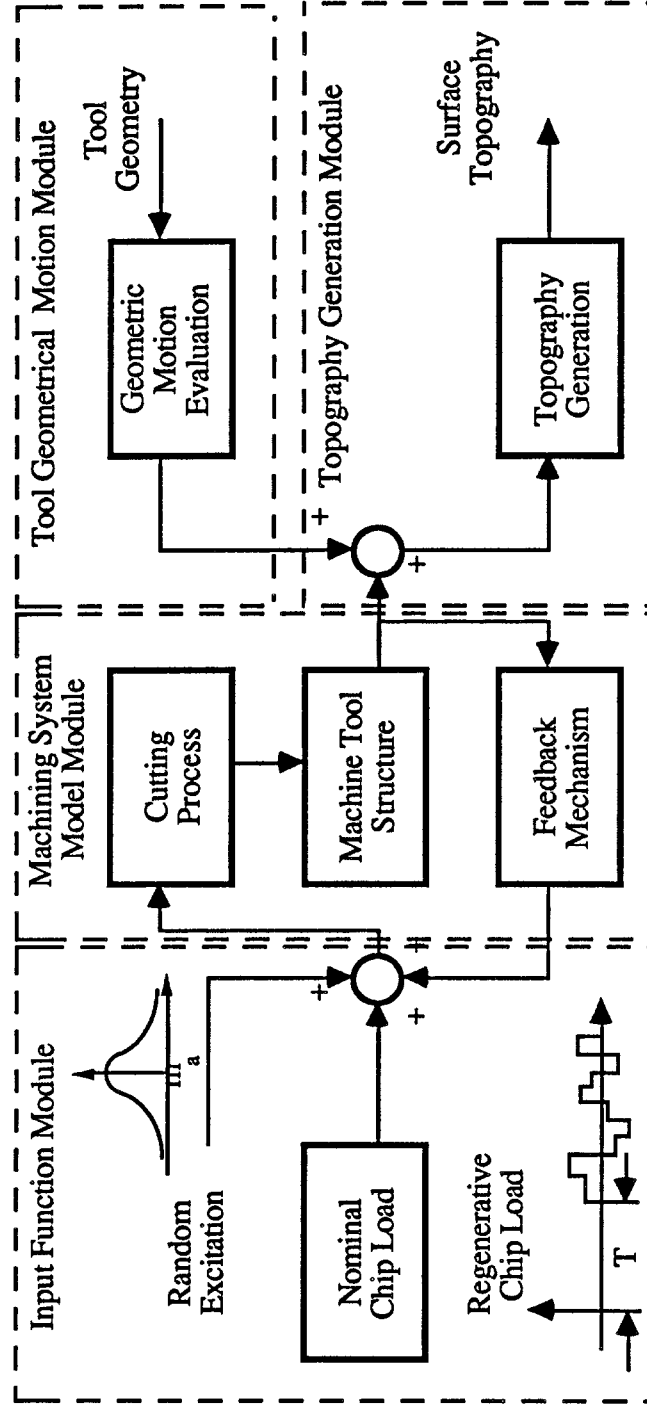


Fig. 2 Methodology to Simulate the Topography of a Machined Surface

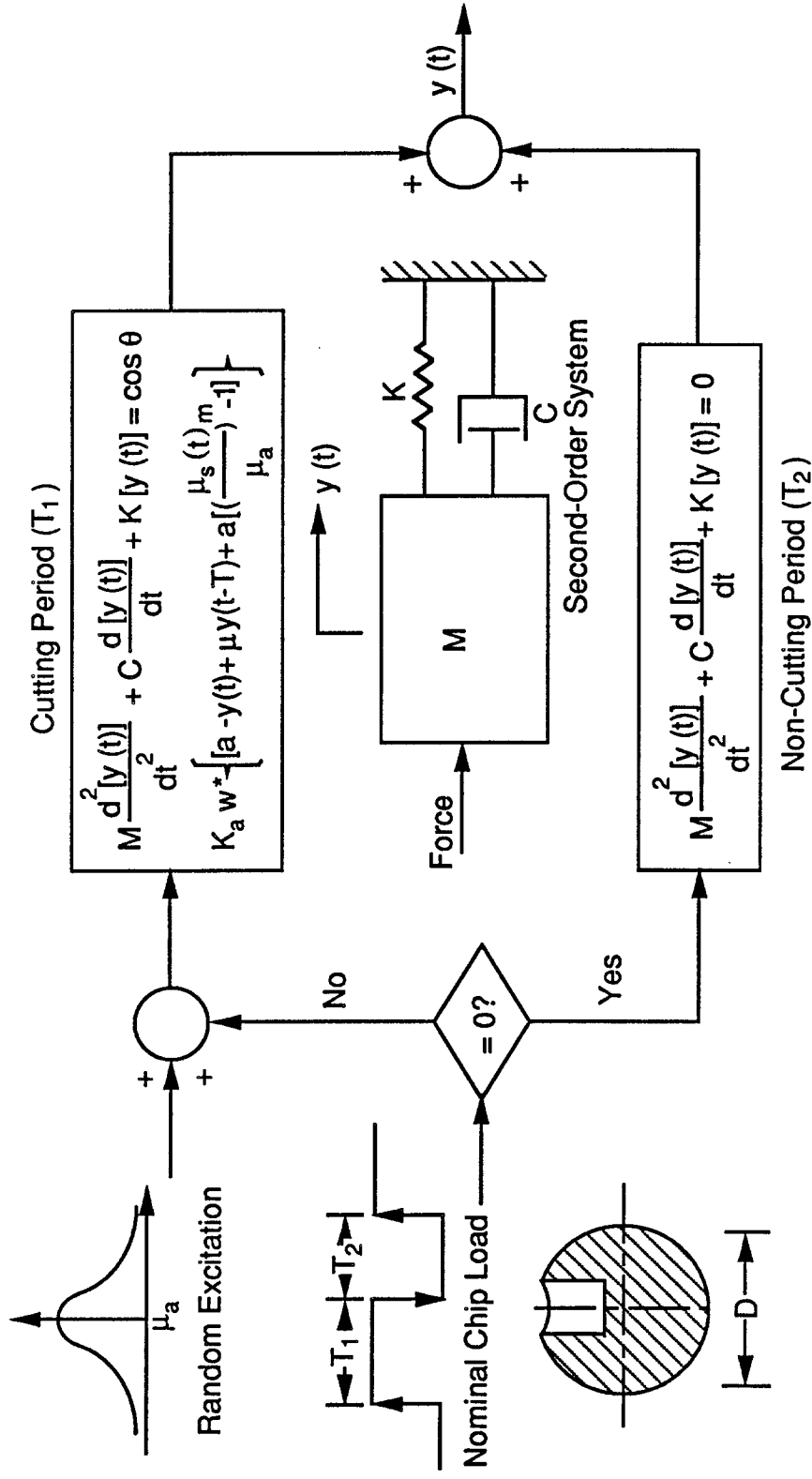


Fig. 3 Machining System Model

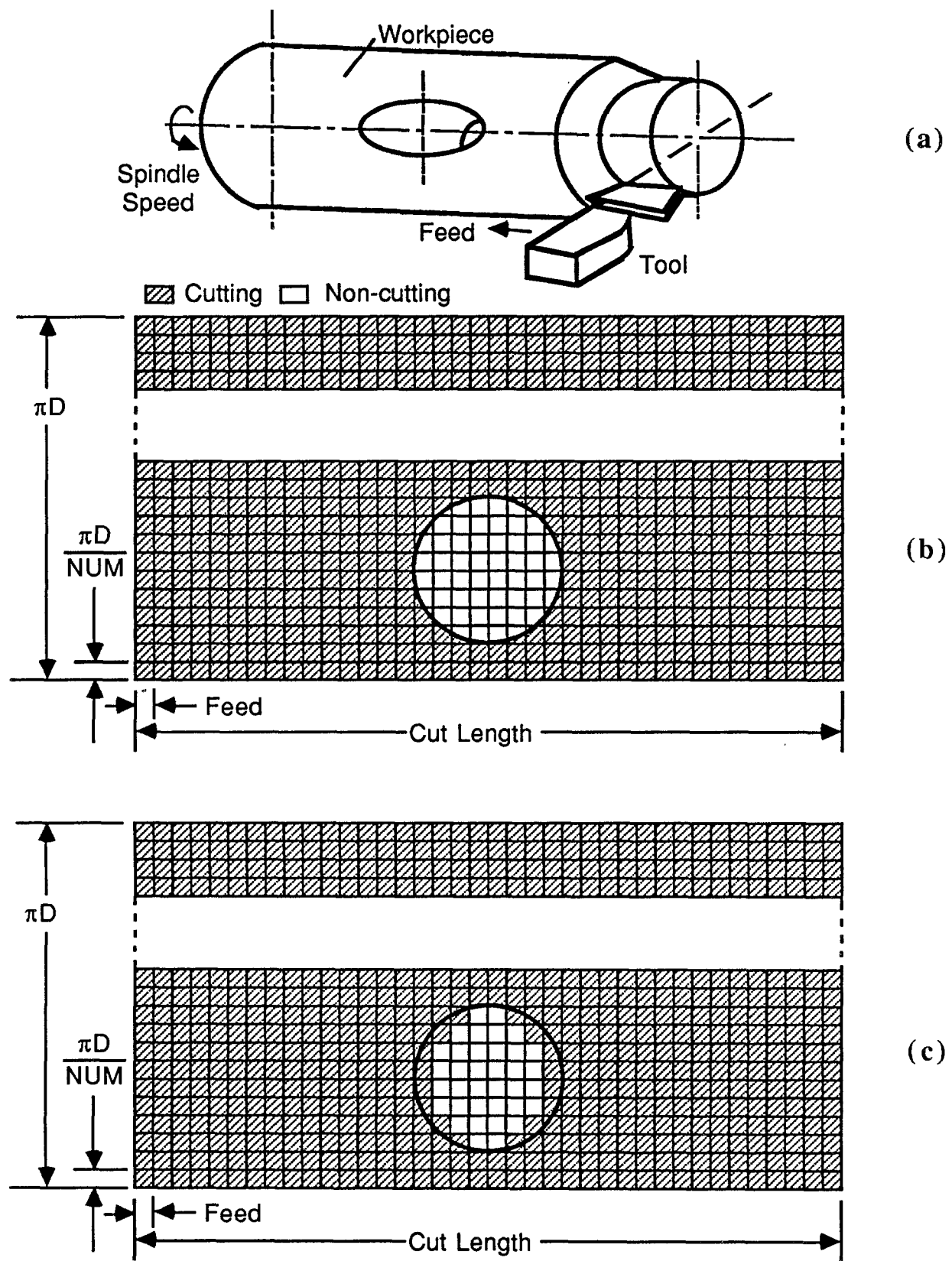


Figure 4 Grid Generator

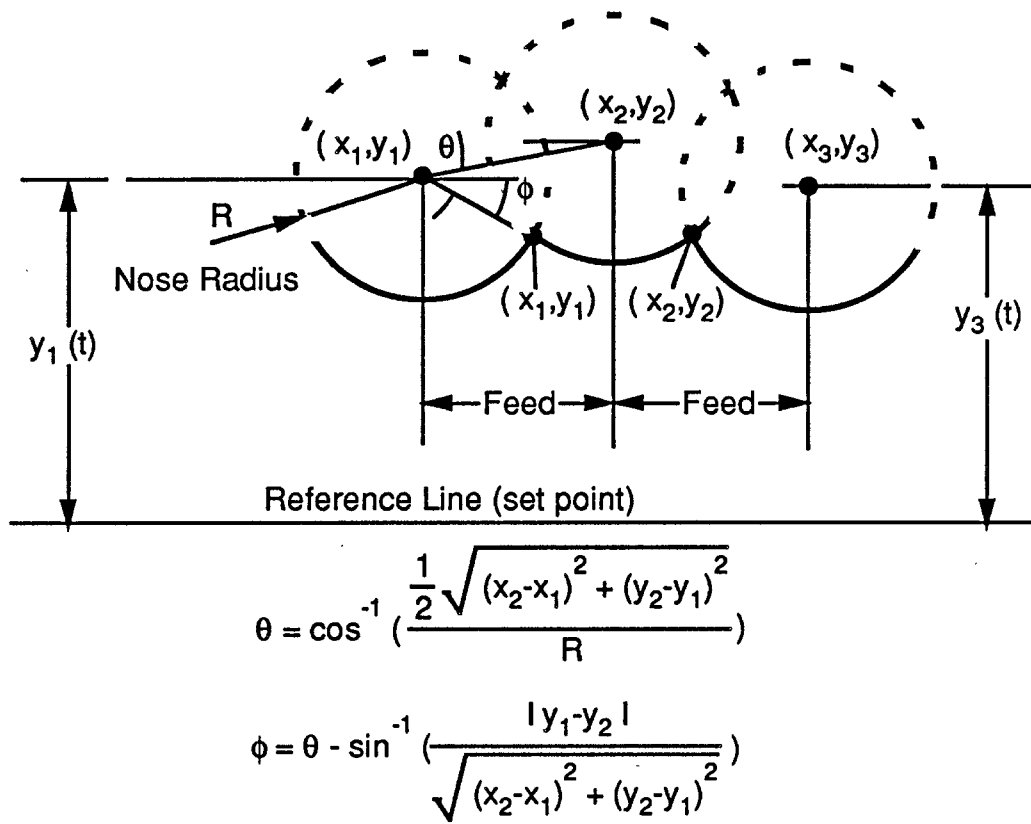
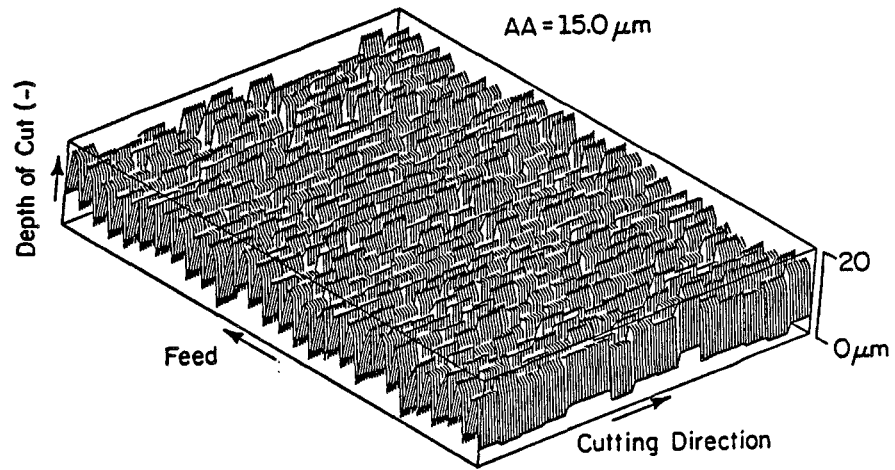
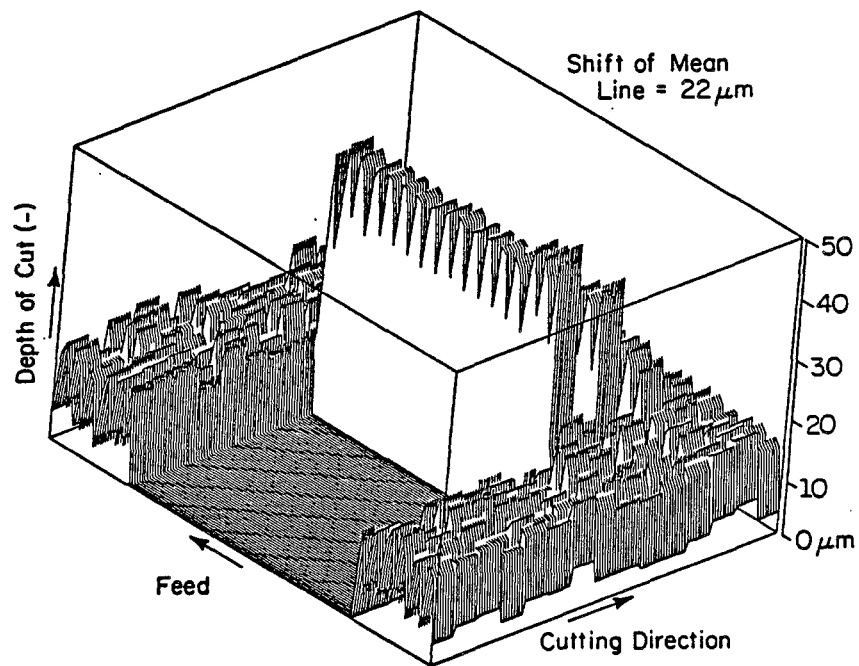


Fig. 5 Construction of a Two - Dimensional Roughness Profile

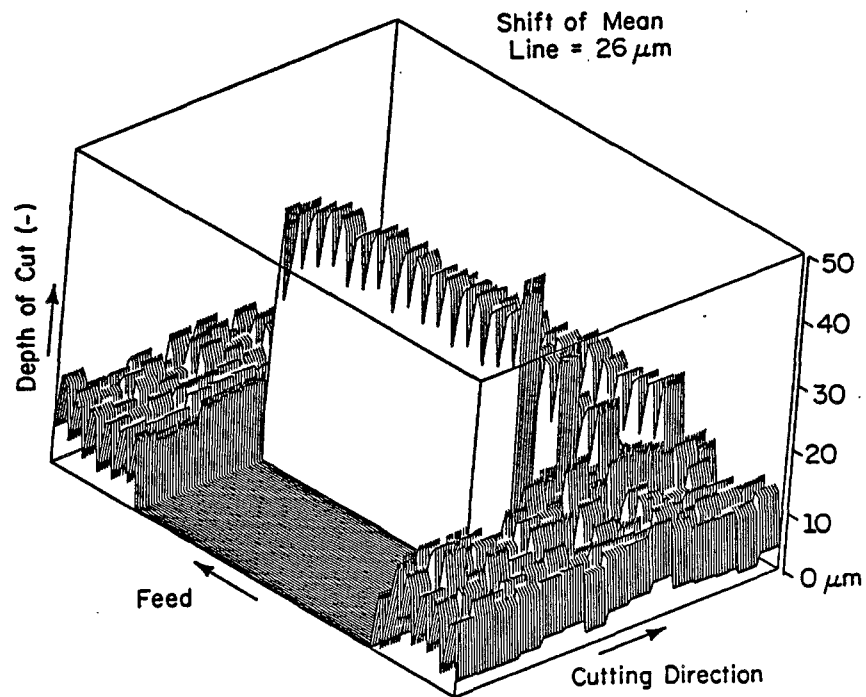


(a). Case 1: Continuous Turning Process

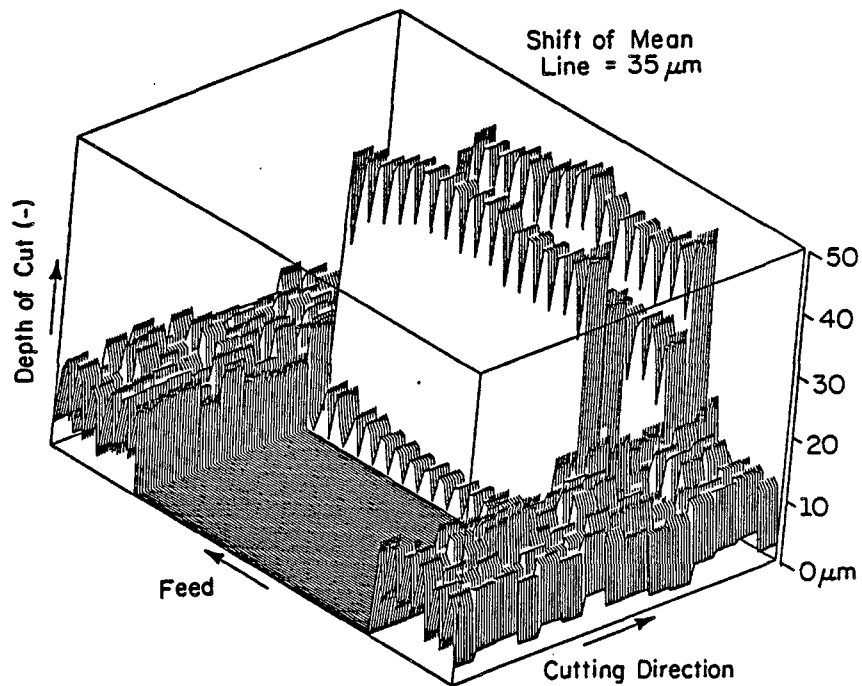


(b). Case 2: Intermittent Turning Process
(Width = 30 mm and 600 rpm)

Figure 6 Topographies Simulated in the Four Case Studies (Continued)

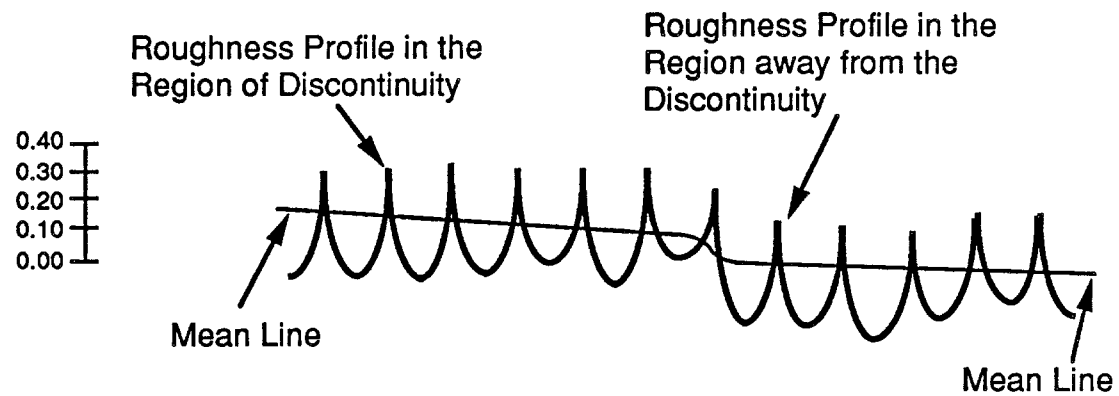


(c). Case 3: Intermittent Turning Process
(Width = 20 mm and 600 rpm)

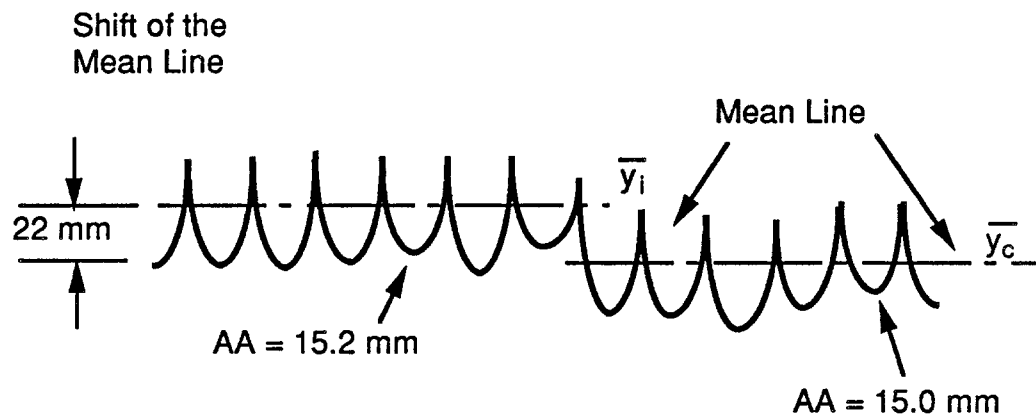


(d). Case 4: Intermittent Turning Process
(Width = 30 mm and 1200 rpm)

Figure 6 Topographies Simulated in the Four Case Studies



(a). A Roughness Profile Consisting of Two Distinct Parts



(b). Definition of the Index - Shift of the Mean Line

Figure 7 Characteristics of Surface Finish after the Intermittent Turning

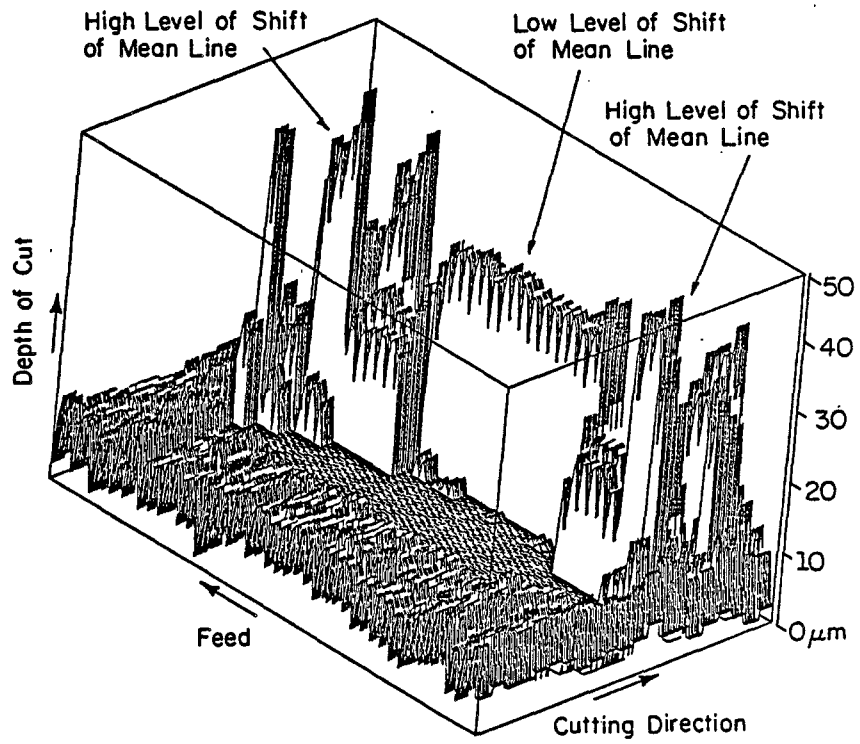


Figure 8 Topography Simulated in Case 5 where a Cylindrical Hole is Located on the Circumference of the Workpiece

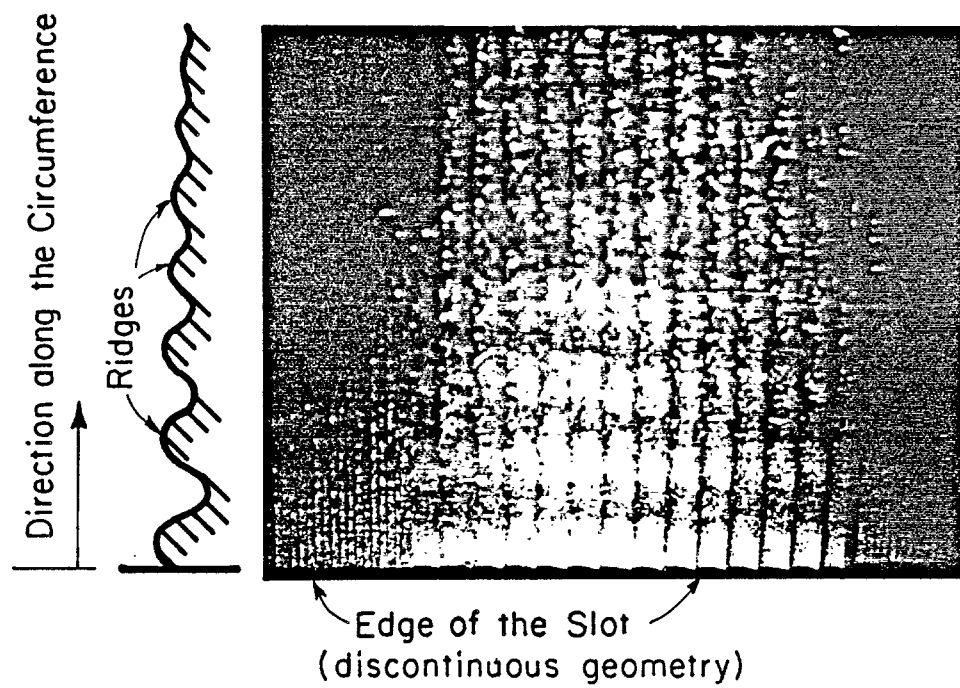


Figure 9 Ridges Formed along the Boundary of Discontinuous Geometry
Observed From Experiment (Magnified 28X)

Table 1 Simulation Conditions Used in the Case Studies

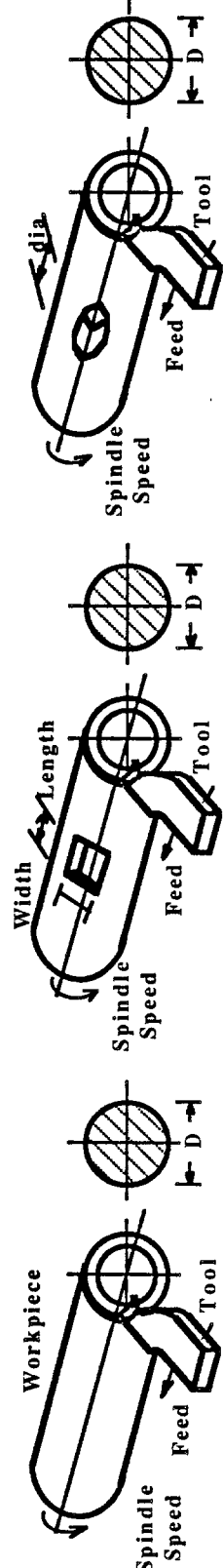
Case	Case 1	Case 2	Case 3	Case 4	Case 5
workpiece Geometry	continuous	discontinuous rectangle width = 30 mm length = 10 mm	discontinuous rectangle width = 20 mm length = 10 mm	discontinuous rectangle width = 30 mm length = 10 mm	discontinuous circle dia. = 25 mm
Topography	Figure 6a	Figure 6b	Figure 6c	Figure 6d	Figure 7a
cutting parameters	Feed mm/rev	0.50	0.50	0.50	0.50
	depth of cut mm	0.60	0.60	0.60	0.60
	spindle speed rpm	600	600	1200	600
					

Table 2 Shift of Mean Line at Different Spindle Speeds

Spindle Speed (rpm)	200	400	600	800	1000	1200
Time Duration of Non-Cutting Period (second)	0.036	0.018	0.012	0.009	0.0072	0.006
Shift of Mean line (um)	20	24	22	30	27	35

